Ferritin But Not Iron Increases in Retina Upon Systemic Iron Overload in Diabetic and Iron-Dextran Injected Mice

Aina Bonet,[1,2] Judit Pampalona,[1] Eduard Jose-Cunilleras,[3] Víctor Nacher,[2] and Jesús Ruberte[1,2]

[1]Centre for Animal Biotechnology and Gene Therapy (CBATEG), Universitat Autònoma de Barcelona, Bellaterra, Spain
[2]Department of Animal Health and Anatomy, Faculty of Veterinary Medicine, Universitat Autònoma de Barcelona, Bellaterra, Spain
[3]Department of Animal Medicine and Surgery, Faculty of Veterinary Medicine, Universitat Autònoma de Barcelona, Bellaterra, Spain

Correspondence: Jesús Ruberte, CBATEG – Center for Animal Biotechnology and Gene Therapy, Autonomous University of Barcelona, C/de la Vall Morona, Bellaterra (Cerdanyola del Vallès) 08193, Spain; jesus.ruberte@uab.cat.

AB and JP contributed equally.

Received: March 8, 2022
Accepted: February 13, 2023
Published: March 13, 2023

Citation: Bonet A, Pampalona J, Jose-Cunilleras E, Nacher V, Ruberte J. Ferritin but not iron increases in retina upon systemic iron overload in diabetic and iron-dextran injected mice. *Invest Ophthalmol Vis Sci.* 2023;64(3):22. https://doi.org/10.1167/iovs.64.3.22

Purpose. Iron overload causes oxidative damage in the retina, and it has been involved in the pathogeny of diabetic retinopathy, which is one of the leading causes of blindness in the adult population worldwide. However, how systemic iron enters the retina during diabetes and the role of blood retinal barrier (BRB) in this process remains unclear.

Methods. The db/db mouse, a well-known model of type 2 diabetes, and a model of systemic iron overload induced by iron dextran intraperitoneal injection, were used. Perls staining and mass spectrophotometry were used to study iron content. Western blot and immunohistochemistry of iron handling proteins were performed to study systemic and retinal iron metabolism. BRB function was assessed by analyzing vascular leakage in fundus angiographies, whole retinas, and retinal sections and by studying the status of tight junctions using transmission electron microscopy and Western blot analysis.

Results. Twenty-week-old db/db mice with systemic iron overload presented ferritin overexpression without iron increase in the retina and did not show any sign of BRB breakdown. These findings were also observed in iron dextran-injected mice. In those animals, after BRB breakdown induced by cryopexy, iron entered massively in the retina.

Conclusions. Our results suggested that BRB protects the retina from excessive iron entry in early stages of diabetic retinopathy. Furthermore, ferritin overexpression before iron increase may prepare the retina for a potential BRB breakdown and iron entry from the systemic circulation.

Keywords: iron overload, ferritin, diabetic retinopathy, BRB breakdown, eye cryopexy

Iron is one of the most abundant elements in the earth's crust and is essential for development and survival of organisms. As a metal, iron has the capacity to donate and accept electrons in redox reactions that are required in vital enzymatic processes such as oxygen transport, energy production, DNA replication, neurotransmitter signaling, myelin shedding, and steroid hormone synthesis.[1] In the retina, iron is a co-factor for RPE65 synthesis, involved in the phototransduction cascade.[2,3] Furthermore, iron-containing enzymes are responsible of the shedding and renewal of the photoreceptor outer segment disc membranes.[4]

After iron absorption in the duodenum, iron is released to the bloodstream and bound to the iron carrier transferrin for tissue delivery. Once in the cell membrane, transferrin binds to its transferrin receptor, and the entire complex enters the cell by endocytosis.[5] Then, iron is used for cellular functions, while excess of iron is stored in ferritin. When needed, iron exits the cells through the iron exporter ferroportin.[6] In addition, it has been described that ferritin can act as an iron importer by binding its L and H subunit to the receptors SCARA5 and TIM2, respectively.[7,8] In fact, our group has showed that this iron import alternative mechanism also works in the retina.[9,10]

In states of iron overload, the iron regulatory proteins (IRPs) initiate a series of mechanisms to protect the cells, increasing the expression of ferritin to store more iron.[11–14] However, when iron levels exceed the limit, free ferrous ion triggers the production of oxygen free radicals via the Fenton reaction, which are toxic and can cause DNA alterations, protein damage, and lipid peroxidation.[17] This can be especially harmful in the retina, which presents a high oxygen tension and metabolic rate.[15]

Diabetes has been widely associated with systemic iron overload.[16,17] Recent studies have showed a positive correlation between iron in serum and the risk of developing diabetes.[18,19] Supporting this association, several mouse models of iron overload have been described to develop retinal lesions resembling diabetic retinopathy.[9,20–22] Furthermore, iron overload in diabetic mouse exacerbates the progression of diabetic retinopathy.[23] Nevertheless, wild-type mice in which iron overload was experimentally induced by iron dextran injection exhibited that systemic iron had

minimal penetration in the retina.[24] Thus the mechanism by which systemic iron overload induces retinal iron overload remains unclear.

The aim of this study is to analyze the relation between systemic and retinal iron during diabetes and the implication of the BRB, as it has been suggested to have a role in the regulation of iron transport into the retina.[24] Clarifying the mechanism of iron entry in the retina could be crucial for the prevention and treatment of diabetic retinopathy, since it is mainly exacerbated by oxidative damage. For this purpose, two mouse models have been used: (i) the db/db mouse, a widely accepted model for type 2 diabetes[25–27] and (ii) iron dextran-injected mice, a model of systemic iron overload.[28,29]

Material and Methods

Mice

Male diabetic mice db/db (BKS.Cg-Dock7^{m} +/+ Lepr^{db}/J), nondiabetic littermates db/+ (BKS.Cg-Dock7^{m} + Lepr^{db}/+) and C57BL/6J wild-type (WT) mice of 20 weeks old were used in this work. The animal facility had a controlled environment (20°C temperature, 60% humidity, and 12 hours light/dark cycles) and mice were fed *ad libitum* with a standard diet (2018S TEKLAD Global; Harlan Teklad, Madison, WI, USA). Mice were euthanized with an overdose of inhaled isoflurane or anesthetized with an injected solution of ketamine (100 mg/kg) and xylazine (12 mg/kg) followed by cervical dislocation. Experiment procedures were performed following the ARVO Statement for the Use of Animals in Ophthalmic and Vision Research and the ARRIVE (Animal Research: Reporting In Vivo Experiments) guidelines 2.0. All the procedures were approved by the Ethics Committee in Animal and Human Experimentation of the Universitat Autònoma de Barcelona (UAB) (FUE-2018-00717286).

Glycaemia Measurement

The db/db mice start to show hyperglycemia at four to eight weeks of age.[30] Glycemia was measured in nonfasted conditions with a glucometer (Bayer, Leverkusen, Germany) in blood collected from the tail vein. Mice were considered diabetic when glycemia values were greater than 250 mg/dL in, at least, in two consecutive measurements. According to this, 20-week-old mice presented a significant statistical difference in body weight (30.21 ± 0.665 g, n = 16, in db/+ vs. 52.69 ± 1.117 g, n = 13, in db/db; $P < 0.0001$) and glycemia (121.2 ± 3.204 mg/dL, n = 16, in db/+ vs. 519.1 ± 21.12 mg/dL, n = 13, in db/db; $P < 0.0001$), confirming that db/db mice used in this study had type 2 diabetes.

Analysis of Iron Parameters in Systemic Blood

Mice were anesthetized using inhaled isoflurane, and blood samples were collected by intracardiac puncture, placed in a lithium heparin tube, and spun in a centrifuge to obtain plasma for biochemistry analysis. Serum iron concentration and unsaturated iron binding capacity were determined with an automated biochemistry analyzer (Chemistry Analyzer AU400; Olympus, Tokyo, Japan) and enzymatic colorimetric assays (Beckman Coulter, Inc, Southfield, MI, USA). Total iron binding capacity (TIBC) was calculated adding serum iron concentration to the unsaturated iron binding capacity values.

Perls Prussian Blue Iron Staining

Perls stain was performed in 3 µm paraffin sections of eyeballs, that were sectioned along their axis, and spleens, that were cut transversally. Samples were deparaffinated, rehydrated, and immersed in a solution of 5% potassium ferrocyanide (Sigma-Aldrich, St Louis, MO, USA) and 5% hydrochloric acid (Panreac Química SLU, Castellar del Vallés, Spain). Nuclear fast red (Sigma-Aldrich) was applied for nuclear counterstaining. Sections were washed, dehydrated, and mounted in DPX medium (Sigma-Aldrich) before analysis. To assess iron content in the spleen, Prussian Blue precipitate was quantified with ImageJ software (National Institutes of Health, Bethesda, MD, USA).

Detection of Total Retinal Iron by Inductively Coupled Plasma Mass Spectrometry (ICP-MS)

Eyes were enucleated and retinas were dissected in 1x phosphate buffered saline (PBS) and collected in vials. A blank with 1x PBS was also included to normalize the values. For retinal digestion, samples were treated with 65% nitric acid and heated at 120°C for 30 minutes. Retinal iron concentration was determined by inductively coupled plasma mass spectrometer Agilent 7500ce (Agilent, Santa Clara, CA, USA).

Injection of Iron Dextran and BRB Breakdown by Cryopexy

To induce acute systemic iron overload, 1g/kg of iron dextran (Sigma-Aldrich) was injected intraperitoneally in WT mice. Saline solution was injected instead of iron dextran in a control group. After 4 hours, animals were anesthetized. BRB breakdown by cryopexy was induced in half of the mice injected with iron dextran, by applying a piece of dry ice in the scleral conjunctiva at the lateral palpebral commissure for 10–20 seconds.[31] Eye and spleen samples were collected for paraffin embedding and eyes for ICP-MS analysis. For ICP-MS analysis, mice were subjected to a vascular washout to prevent measuring the iron inside the retinal blood vessels, which could modify the results of iron content in the retinal parenchyma homogenates. For this purpose, thorax was opened to expose the heart, 2 ml 1x PBS were injected in the left ventricle, and the caudal vena cava was cut to interrupt venous return.

Assessment of BRB Breakdown by Evans Blue and Bis-Benzimide

Evans Blue and bis-benzamide (Hoechst) were used to validate BRB breakdown after cryopexy performed on the right eye of Ketamine-Xylazine anesthetized mice (100 mg/kg and 12 mg/kg, respectively). The left eye was used as a control. Thirty minutes after cryopexy, the thorax of the anesthetized mice was opened to expose the heart and 0.5 ml of a solution containing Evans blue 8% and bis-benzamide (1 mg/ml) was injected directly into the left ventricle. Then, the eye was enucleated, and the retina dissected in 1xPBS for vessel visualization and image analysis under the microscope (Nikon Eclipse, E800), using the ACT-1 software. Heparin (10 u/gr) was injected prior injection to prevent blood coagulation.

Investigative Ophthalmology & Visual Science

Western Blot

Retina and spleen samples were homogenized in RIPA buffer with a protease inhibitor (Roche, Basel, Switzerland). For sample preparation, 50 mg of protein were resuspended in 2x Laemmli loading buffer (pH 6.7) (Sigma-Aldrich) and heated at 95°C for 5 minutes. Electrophoresis was performed by loading 12 µL of sample in a 12% pre-cast SDS-PAGE gel (Bio-Rad Laboratories, Hercules, CA, USA), which was later transferred to a polyvinylidene difluoride (PVDF) membrane (Merck Millipore, Billerica, MA, USA). After 1 hour blocking with either 5% non-fat dried milk or 2% bovine serum albumin (Sigma-Aldrich) in Tris buffered saline, 0.05% Tween 20, membranes were incubated overnight at 4°C with the following primary antibodies: rabbit anti-mouse L-ferritin (1:1000; ab69090, Abcam, Cambridge, UK); rabbit anti-mouse H-ferritin (1:1000; ab65080, Abcam); rabbit anti-mouse SCARA5 (1:1000; ab76720, Abcam); rabbit anti-mouse transferrin (1:2000; PA3-913, Thermo Fisher Scientific, Wilmington, DE, USA); rat anti-mouse transferrin receptor (1:1000; ab63333, Abcam); rabbit anti-mouse claudin-5 (1:1000; 34-1600, Thermo Fisher Scientific); and rabbit anti-mouse VEGF (1:100; ab46154, Abcam). For protein normalization, rabbit anti-mouse α-tubulin (1:80000; ab4074, Abcam) or rabbit anti-human α smooth muscle actin (1:10000; ab5694, Abcam) were used as a loading control. Secondary antibodies goat anti-rabbit (Bionova Scientific, Fremont, CA, USA) and sheep anti-rat (LifeSpan, Providence, RI, USA) horseradish peroxidase at 1:5000, were used. Immobilon Crescendo Western HRP Substrate (Merck Millipore) and the ImageJ software were used for band detection and quantification, respectively.

Immunohistochemistry

Paraffin embedded mice eyes and spleens were sectioned, deparaffinized, and rehydrated. Antigen retrieval was performed in a solution with 3.38% citric acid and 24.4% sodium citrate. Sections were washed in PBI (1x PBS, 0.05% Igepal). The following primary antibodies were used: rabbit anti-mouse L-ferritin (1:100; ab69090 Abcam); rabbit anti-mouse H-ferritin (1:100; ab65080 and ab183781 Abcam); goat anti-mouse collagen IV (1:20; AB769, Merck Millipore); and rabbit anti-mouse albumin (1:2000; A001, DAKO, Glostrup, Denmark). All primary antibodies were diluted in 1x PBS, 0.5% bovine serum albumin, 0.05% Igepal with 10% of donkey serum (Sigma Aldrich), except anti-albumin antibody that was diluted in PBI. Negative controls were included by omitting the primary antibody in sequential tissue sections. Secondary antibodies donkey anti-goat Alexa 488 (1:1000; Life Technology, Carlsbad, Ca, USA) and goat anti-rabbit 568 (1:1000; Invitrogen, Carlsbad, CA, USA) were incubated for 2 hours. Samples were counterstained with Hoechst (Sigma-Aldrich), mounted in Fluoromount (Sigma-Aldrich) and analyzed in a SP5 laser scanning confocal microscope (Leica Microsystems GmbH).

In Vivo Observation of Eye Fundus Vascularization

Mice were anaesthetized with an intraperitoneal injection of a ketamine and xylazine cocktail. During anesthesia, Viscofresh (Allergan, Dublin, Ireland) was applied in the eyes to prevent them from drying. Eye drops of tropicamide (Alcon, Barcelona, Spain) were used to induce mydriasis, and 10 µl of 5% sodium fluorescein (Sigma-Aldrich) were injected subcutaneously in each mouse to observe the eye fundus vascularization. Custom-made mouse lenses were placed on the corneas while visualizing retinal blood vessels in the HRA2 scanning laser ophthalmoscope (Heidelberg Engineering, Heidelberg, Germany). Angiography was performed in both eyes and in the three retinal vascular plexi.

Transmission Electron Microscopy (TEM)

Retinas were dissected in 1x PBS and cut into 1 mm^2 fragments. Retinal fragments were fixed in 2,5% glutaraldehyde and 2% paraformaldehyde for 2 hours at 4°C and then washed in PBI. Post fixation was performed with 1% osmium tetroxide for 2 hours. Samples were dehydrated in a graded acetone solution and infiltrated with Spurr resin (Sigma-Aldrich). Ultra-sections of 60–80 nm were obtained with ultramicrotome Leica EM UC6 and contrasted with Reynolds' stain and 2% aqueous uranyl acetate. Finally, samples were analyzed with a transmission electron microscope Jeol JEM-1400 (Jeol Ltd., Tokyo, Japan).

Retinal Thickness Measurement

To evaluate retinal thickening, an indicator of retinal oedema,[32] paraffined eyes were sectioned through their axis and were stained with hematoxylin and eosin. Retinal thickness was measured between the internal limiting membrane and the outer limiting membrane. A total of six areas, at 100 µm, 500 µm, and 1000 µm on each side of the optic nerve head, were analyzed. ImageJ was used for morphometric analysis by an operator blinded to the experimental groups.

Statistical Analysis

For statistical analyses R Software (version 4.1.0; R Foundation for Statistical Computing, Vienna, Austria) was used. Shapiro-Wilk test was performed for evaluation of the data distribution and F test for the variance homogeneity. Data with normal distribution was analyzed using the parametric method unpaired *t*-test and data not normally distributed was analyzed with Wilcoxon test. Data are expressed as mean ± standard error of the mean (SEM). Differences between groups were considered significant at P-value$<$0.05.

Results

Systemic Iron Was Increased in 20-Week-Old Diabetic Mice

To assess systemic iron status in diabetic mice we first analyzed the iron content in the spleen using Perls stain. The results revealed that db/db mice presented a significant increase of iron content compared to db/+ (0.452 ± 0.136 arbitrary units (au) in db/+ mice vs. 1.489 ± 0.387 au in db/db mice; p = 0.0142; n = 9) (Fig. 1A). As expected, iron was mostly accumulated in the red pulp (Fig. 1A), where erythrophagocytosis takes place. Another widely used indicator to assess iron content in tissues is ferritin concentration.[33–35] To assess if the increment of iron in db/db spleen correlated with a higher L-ferritin expression, western

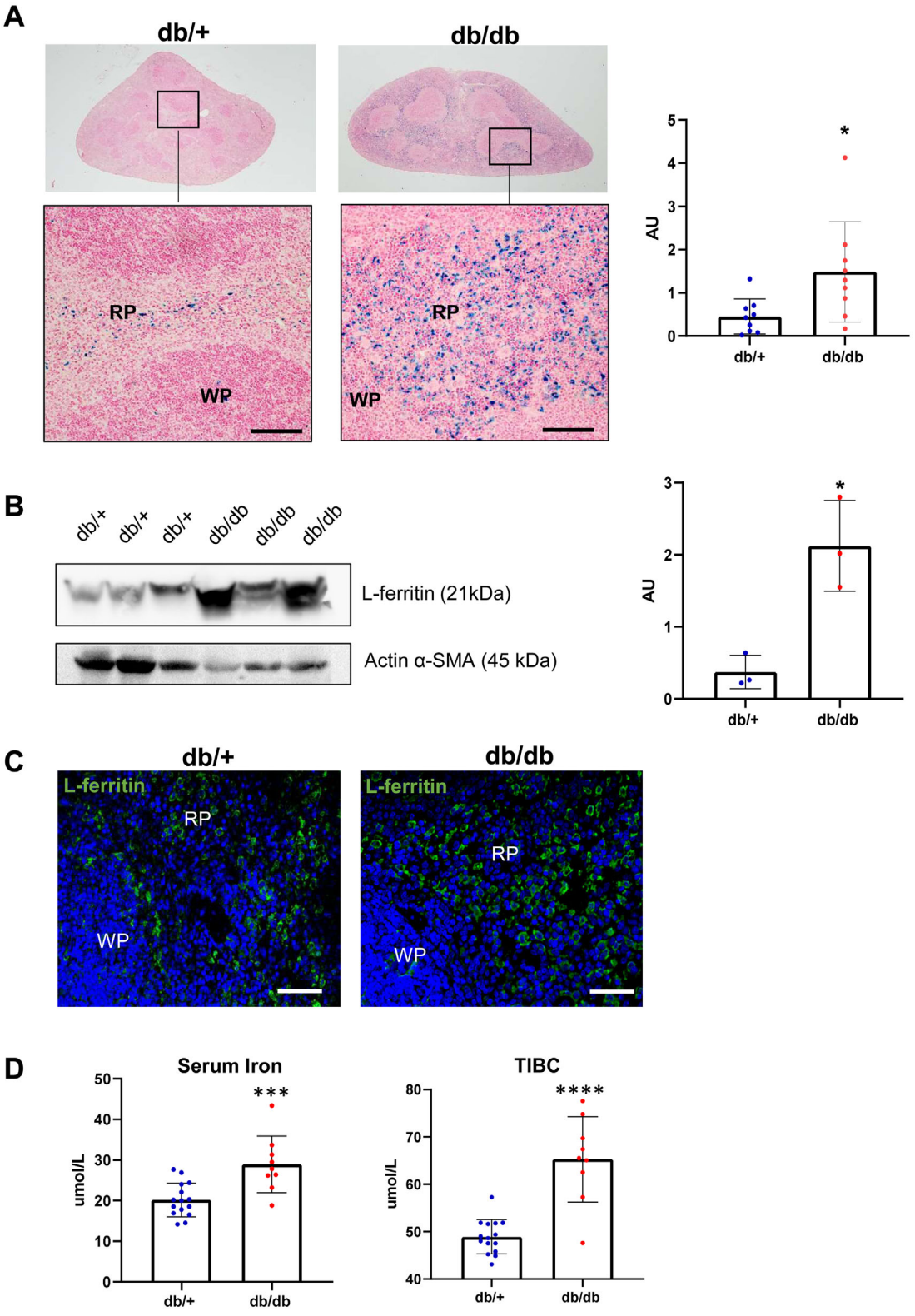

Figure 1. Spleen and serum iron, TIBC and spleen ferritin were increased in 20-week-old db/db mice. (**A**) Perls stain showed a significant increment in iron content in the spleen of db/db mice, mostly in the red pulp. (**B**) Western blot analysis also revealed higher levels of L-ferritin expression in spleen of db/db mice. α-smooth muscle actin was used as a loading control. (**C**) Immunofluorescence representative images showed increased L-ferritin expression in the red pulp of db/db mouse spleen. Nuclei were counterstained with Hoechst. (**D**) Serum iron and TIBC, which is an indicator of serum transferrin concentration, were significatively increased in db/db mice. RP: red pulp; WP: white pulp. *$P < 0.01$; ***$P < 0.001$; ****$P < 0.0001$, respectively. *Scale bar:* 100 µm (**inset A**), 30 µm (**C**).

Investigative Ophthalmology & Visual Science

blot was performed and as expected, db/db mice exhibited higher amounts of L- ferritin (0.372 ± 0.133 au in db/+ mice vs. 2.123 ± 0.364 au in db/db mice; p = 0.0107; n = 3) (Fig. 1B). Immunohistochemistry showed that the increase of L-ferritin expression occurred also in the red pulp, where iron is accumulated (Fig. 1C).

The increment in iron and ferritin content found in the db/db mouse spleen showed concordance with the high levels of serum iron (20.17 ± 1.072 µmol/L in db/+, n = 15 vs. 28.92 ± 2.323 µmol/L in db/db, n = 9; p = 0.0008) (Fig. 1D). This finding was accompanied by an increase of serum TIBC in db/db mice (48.90 ± 0.932 µmol/L in db/+, n = 15 vs. 65.28 ± 3.006 µmol/L in db/db, n = 9; $P < 0.0001$; Fig. 1D), which is an indicator of serum transferrin concentration and iron delivery into the tissues.[36]

Retinas Showed Increased Ferritin, But Not Iron Overload in 20-Week-Old Diabetic Mice

To assess if, as happened in the spleen, retinas from diabetic mice presented an elevated expression of ferritin, levels of both L- and H-ferritin were analyzed by Western blot analysis in db/+ and db/db retinas. An increase of twofold change in L-ferritin (0.484 ± 0.488 au in db/+ vs. 0.9947 ± 0.146 au in db/db; n = 3; $P = 0.029$) and a 3.3-fold change in H-ferritin (0.3168 ± 0.051 au in db/+ vs. 0.986 ± 0.052 au in db/db; n = 3; $P = 0.0008$) were observed in diabetic retinas (Fig. 2A). Immunohistochemistry confirmed an increase in the expression of both ferritin subunits in diabetic retinas (Fig. 2B). L-ferritin immunohistochemistry was quantified in terms of pixel intensity showing a significant increase in the db/db mouse retinas (0.08152 ± 0.0082 db/+, n = 8, vs. 0.1145 ± 0.0094 in db/db, n = 6; $P = 0.02$; Fig. 2C). These results agreed with those obtained by a recent study.[23]

Because Perl's stain was not sensitive enough to detect iron in db/+ and db/db retinas (Supplementary Fig), ICP-MS was used to ensure that retinal ferritin levels correlated with iron levels. Unexpectedly, ICP-MS analysis did not show any difference in the iron content between db/+ and db/db retinas (2.264 ± 0.212 µg iron/g retina in db/+ vs. 2.162 ± 0.071 µg iron/g retina in db/db; n = 5; $P = 0.744$) (Fig. 2D), revealing that increased retinal ferritin was not accompanied with increased iron content in the diabetic retina.

Iron Import Proteins Were Not Increased in 20-Week-Old Diabetic Mouse Retinas

Because ferritin expression, but not iron content, was increased in the retina, we next analyzed the proteins involved in iron import within the retina. In two independent experiments, Western blot analysis showed that transferrin (1.013 ± 0.071 au in db/+ vs. 1.079 ± 0.12 au in db/db; n = 3; $P = 0.665$, in Figure 3A and 1.393 ± 0.156 au in db/+, n = 3, vs. 1.399 ± 0.202 au in db/db; n = 4; $P = 0.985$, in Supplementary Fig. SB) was not increased in diabetic retinas. Similarly, transferrin receptor was also not increased (1.079 ± 0.237 au in db/+ vs. 0.773 ± 0.058 au in db/db; n = 3; $P = 0.278$, in Figure 3A and 0.217 ± 0.004 au in db/+ vs. 0.232 ± 0.013 in db/db; n = 4; $P = 0.313$, in Supplementary Fig. SB). In addition, the receptor of circulating L-ferritin, SCARA5, known to mediate iron import into the retina[10] was also not increased in diabetic retinas (0.9799 ± 0.076 au in db/+ vs. 1.099 ± 0.087 au in db/db; n = 3; $P = 0.363$) (Fig. 3A). Altogether, these results showed that, despite the systemic iron overload and the increase of ferritin, the iron levels and the iron import machinery were not incremented in diabetic retinas, thus suggesting the existence of a mechanism that protects the retina from massive iron entry.

BRB Breakdown Signs Were Not Observed in 20-Week-Old Diabetic Mice

The db/db mice develop complete BRB breakdown at 15 months of age.[37] To assess BRB integrity in 20-week-old diabetic mice, we first analyzed eye fundus with Scanning Laser Ophthalmoscopy (SLO), which revealed that injected fluorescein remained inside the vessels and none of db/+ nor db/db mice presented vascular leakage (n = 16) (Fig. 3B). In addition, serum albumin detected by immunohistochemistry was confined to the vessel lumen, indicating the absence of retinal edema in 20-week-old diabetic mice (Fig. 3C). VEGF, which increases vascular permeability in diabetic retinopathy[38], was also analyzed by Western blot analysis, and no statistical differences were found between db/+ and db/db retinas (1.003 ± 0.142 au in db/+ vs. 0.8553 ± 0.183 au in db/db; n = 3; $P = 0.559$) (Fig. 3D). Furthermore, the comparison of retinal thickness between db/+ and db/db mice confirmed that diabetic retinas did not present edema (183.38 ± 2.102 µm in db/+, n = 12 vs. 187.12 ± 4.696 µm in db/db; n = 6; $P = 0.41$) (Fig. 4A).

Next, to evaluate tight junctions, the key player in the maintenance of BRB integrity[39], ultrathin sections of the retina were analyzed by TEM. Endothelial tight junctions in db/db retinas appeared morphologically normal, without any open space between membranes of neighboring endothelial cells and with the characteristic electron density produced by the tight junction proteins (Fig. 4B). Additionally, one of the most important tight junction proteins in the BRB, claudin-5[40] was analyzed by Western blot analysis. No differences in claudin-5 expression were observed when comparing db/+ with db/db retinas (0.989 ± 0.134 AU in db/+ vs. 1.058 ± 0.243 AU in db/db; n = 3; $P = 0.818$) (Fig. 4C). Altogether, these results showed that BRB was intact in 20-week-old diabetic mice and that could be preventing the entrance of high amounts of circulating iron into the retina.

BRB Protected Retina From Iron Entrance During Systemic Iron Overload

To assess the BRB role in the protection of the retina during iron overload, we experimentally induced systemic iron overload by injection iron dextran intraperitoneally to C57BL/6J WT mice. At four hours after injection, iron accumulation in the spleen was quantified with Perls staining, which demonstrated that iron dextran-injected mice presented systemic iron overload (0.8051 ± 0.46 au in the group injected with saline solution vs. 2.281 ± 0.13 au in the group injected with iron dextran; n = 3; $P = 0.037$) (Fig. 5A). In contrast, Perls staining performed in the retina of dextran-injected mice only detected iron inside the blood vessels and not in the parenchyma (Fig. 5B). ICP-MS confirmed that no statistical differences were found in iron content in the retinal parenchyma between groups (1.768 ± 0.521 µg iron/g retina in saline solution–injected

Investigative Ophthalmology & Visual Science

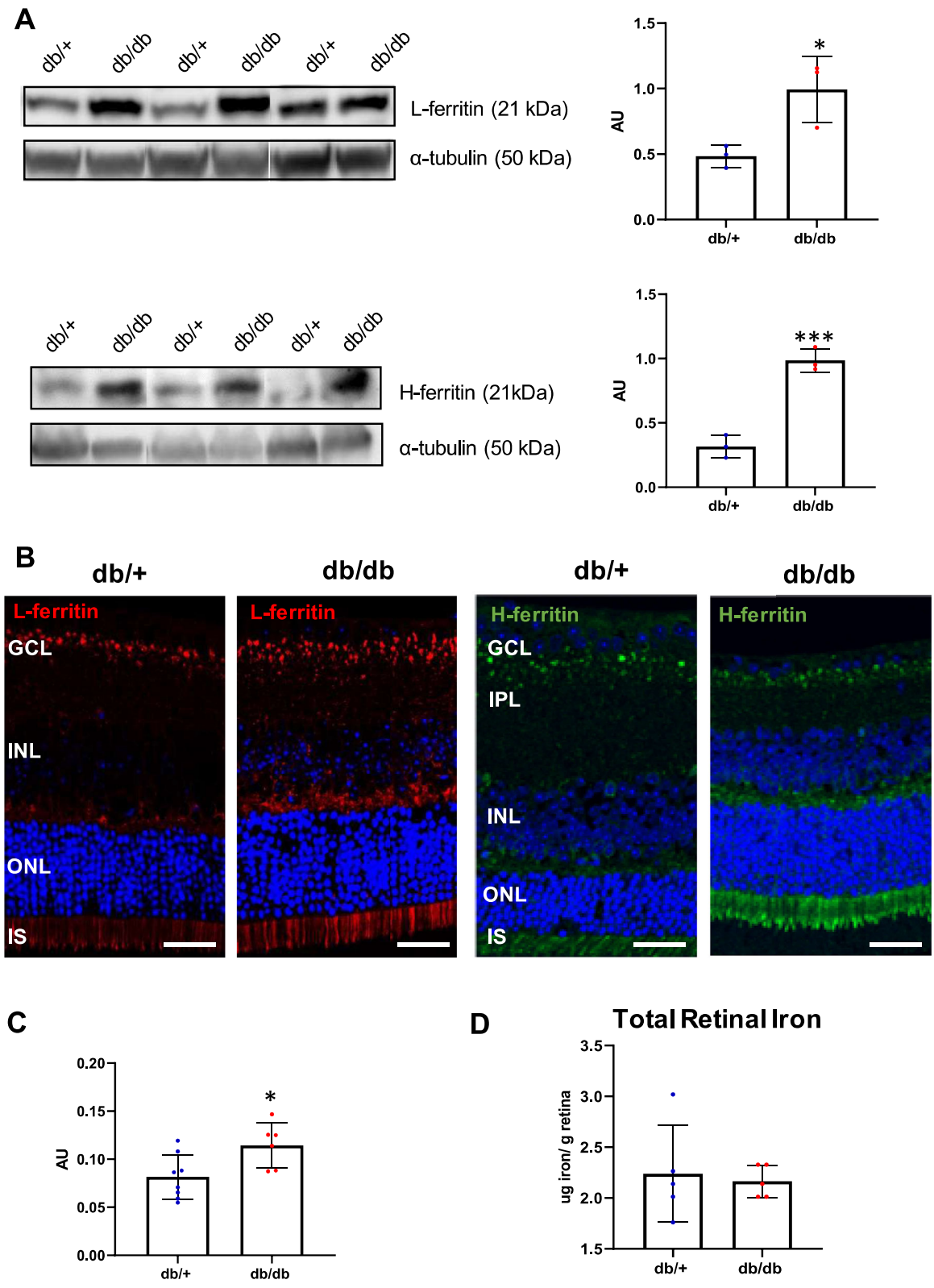

Figure 2. L- and H-ferritin, but not iron, were increased in 20-week-old db/db mouse retinas. (**A**) Western blot analysis revealed that L-ferritin expression was twofold increased and H-ferritin was 3.3-fold increased in db/db mouse retinas. As a loading control, α-tubulin was used. (**B**) Immunofluorescence representative images showed an increase in both L- and H-ferritin expression in db/db mouse retinas. (**C**) L-ferritin immunohistochemistry was quantified in terms of pixel intensity showing higher levels of ferritin in the db/db mouse retinas. Nuclei were counterstained with Hoechst. (**D**) There were no differences between db/+ and db/db retinas in total iron content analyzed with ICP-MS. GCL, ganglion cell layer; IPL, inner plexiform layer; INL, inner nuclear layer; OPL, outer plexiform layer; ONL, outer nuclear layer; IS, inner segments of photoreceptors. *$P < 0.05$; ***$P < 0.001$. *Scale bar*: 32.05 µm.

Investigative Ophthalmology & Visual Science

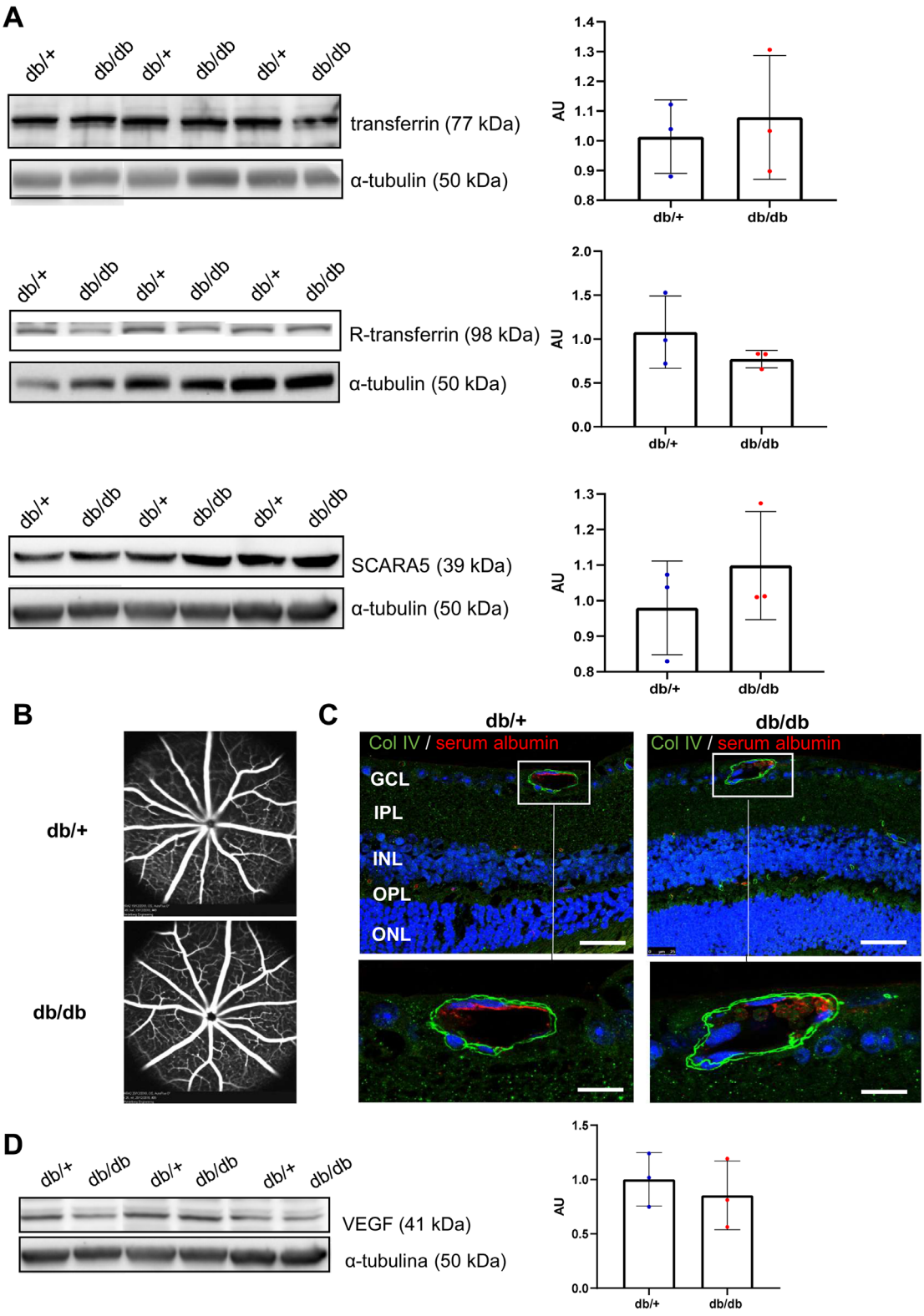

Figure 3. Iron import proteins were not increased, and no signs of BRB breakdown were found in 20-week-old db/db mouse retinas. (**A**) Western blot analysis revealed that neither transferrin nor its receptor was increased in db/db mouse retinas. SCARA5, the receptor of L-ferritin, was also not increased in db/db mouse retinas. As a loading control, α-tubulin was used. (**B**) Analysis of the eye fundus by Scanning Laser Ophthalmoscopy (SLO) showed that injected fluorescein remained inside the retinal blood vessels in db/db mice showing no vascular leakage (n = 16). (**C**) To assess retinal vessels leakage microscopically, immunohistochemistry against serum albumin and collagen IV, a marker for blood basement membrane, was performed. The results showed that serum albumin was restricted inside the vessel lumen in db/db mice. (**D**) Western blot analysis of VEGF expression, which induces vascular permeability, showed no statistical differences between db/+ and db/db retinas. As a loading control, α-tubulin was used. GCL, ganglion cell layer; IPL, inner plexiform layer; INL, inner nuclear layer; OPL, outer plexiform layer; ONL, outer nuclear layer. *Scale bar*: 29.41 µm (**inset:** 11.49 µm).

Investigative Ophthalmology & Visual Science

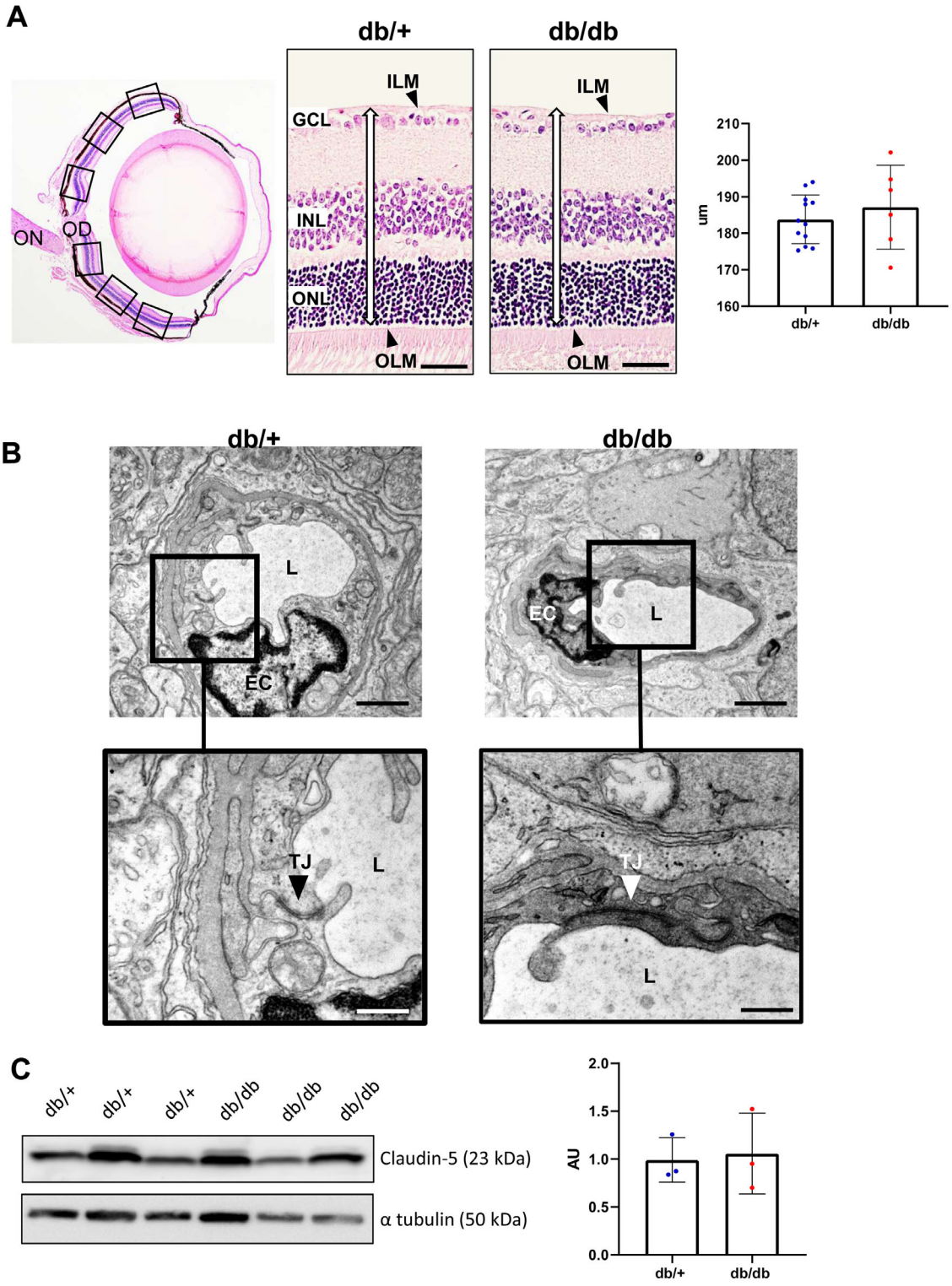

Figure 4. No alterations in thickness and ultrastructure were found in 20-week-old db/db mouse retinas. (**A**) To assess retinal edema, paraffined sections stained with hematoxylin and eosin were measured from the internal limiting membrane to the outer limiting membrane (*arrowheads*) in six different areas (at 100 µm, 500 µm, and 1000 µm on each side of the optic nerve head), and no differences between db/+ and db/db were found. (**B**) TEM analysis revealed a normal ultrastructure and electron density of tight junctions (*arrows*) in db/db retinal vessels. (**C**) Western blot analysis did not show changes in the expression of the tight junction protein claudin-5 in db/db mice retinas. As a loading control, α-tubulin was used. OD, optic disc; ON, optic nerve; GCL, ganglion cell layer; INL, inner nuclear layer; ONL, outer nuclear layer; ILM, internal limiting membrane; OLM, outer nuclear membrane. *Scale bar*: 41.15 µm. EC, endothelial cell; L, vessel lumen; *TJ*, tight junction. *Scale bar*: 41.15 µm in **A**, 200 nm in **B** (**inset:** 217 nm).

Investigative Ophthalmology & Visual Science

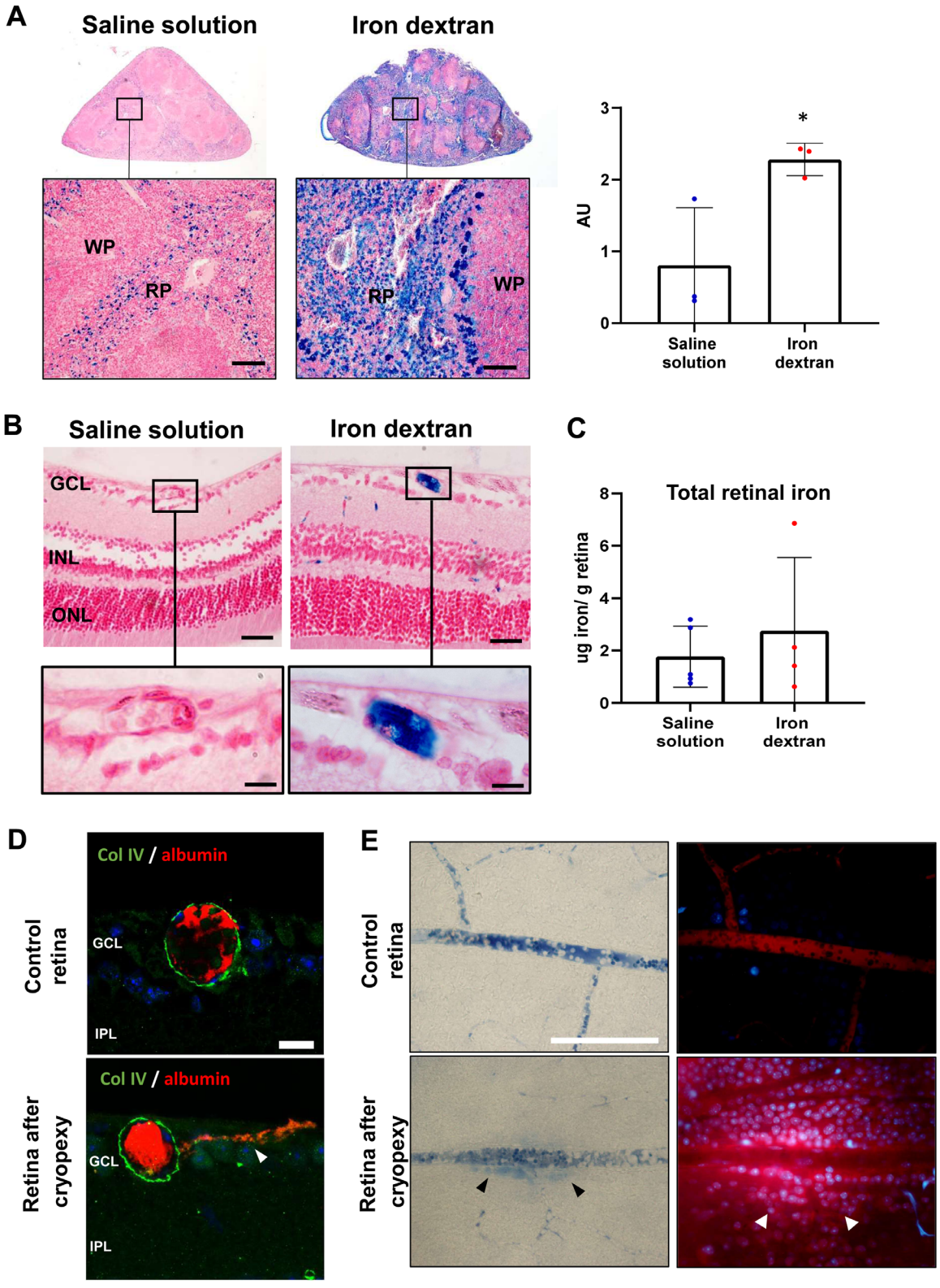

Figure 5. Intraperitoneal injection of iron dextran induced acute systemic iron overload but did not cause retinal iron overload in WT mice. (**A**) At four hours after injection, Perls staining was performed in the mouse spleen showing an increase in iron accumulation in the red pulp of mice injected with iron dextran. (**B**) However, in the retina, Perls stain revealed iron exclusively inside the blood vessels but not in the retinal parenchyma. (**C**) After a vascular washout to remove intravascular iron dextran, ICP-MS was used to quantify iron. (**D**) Only after BRB breakdown was induced by cryopexy, immunohistochemistry against serum albumin and collagen IV showed vascular leakage (*arrowhead*), demonstrating BRB breakdown in retinas from cryopexed eyes. (**E**) injection of Evans blue together with bis-benzamide revealed leakage outside the blood vessel in cryopexed eyes, in blue (*arrowheads* in the bottom left image) and red (*arrowheads* in bottom right image), respectively. Bis-benzamide stained cell nuclei. RP, red pulp; WP, white pulp; GCL, ganglion cell layer; IPL, inner plexiform layer; INL, inner nuclear layer; ONL, outer nuclear layer. *$P < 0.05$. *Scale bar*: 82 µm in **A**, 36.49 µm in **B** (**inset:** 10 µm), 13.7 µm in **D**, and 35.09 in **E**.

Investigative Ophthalmology & Visual Science

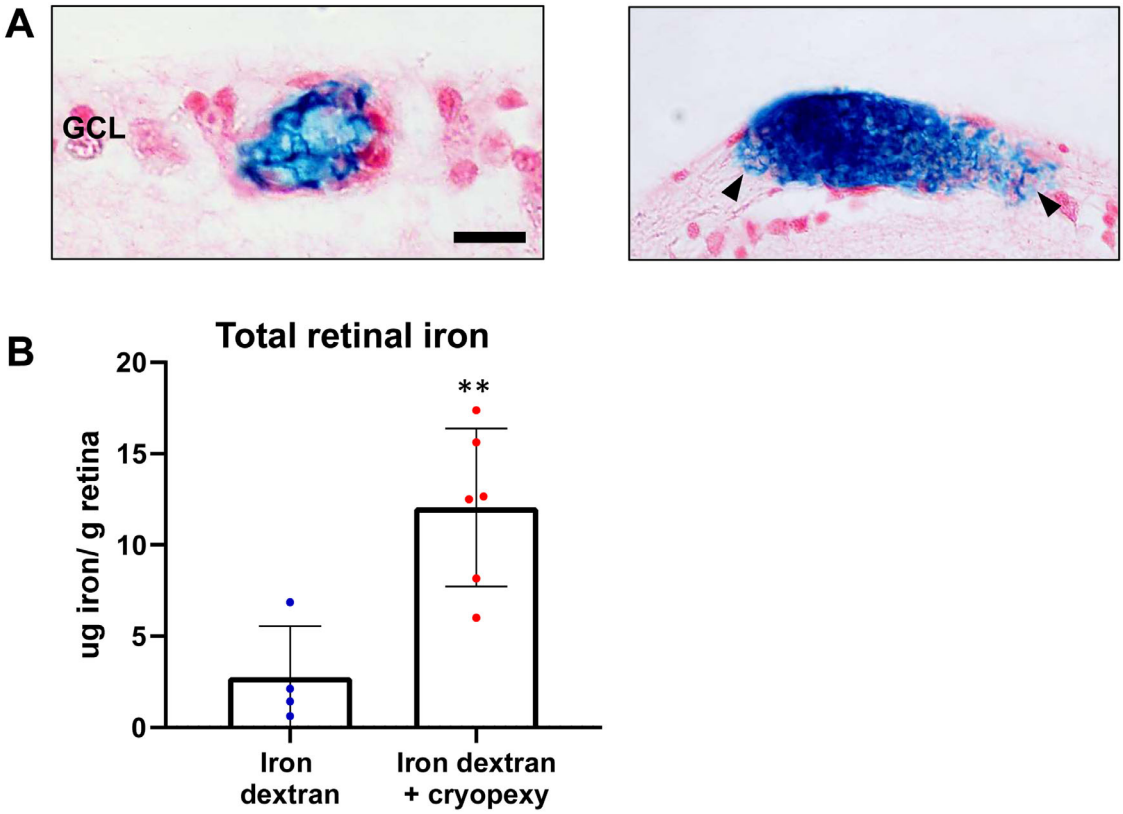

Figure 6. BRB breakdown induced by cryopexy caused retinal iron overload in mice injected with iron dextran. (**A**) Perls staining in paraffin sections showed iron leakage (*arrowheads*) into the retinal parenchyma in cryopexed eyes. (**B**) ICP-MS was used to quantify iron content in the retinal parenchyma, showing, as expected, an increase in retinal iron in cryopexed eyes. GCL, ganglion cell layer. $^{**}P < 0.01$. *Scale bar*: 22.72 µm.

mice, n = 5, vs. 2.755 ± 1.4 µg iron/g retina in the iron dextran-injected mice; n = 4; $P = 0.905$) (Fig. 5C). Altogether, these results supported the hypothesis that the BRB has a protective effect in preventing retinal iron overload.

Finally, to confirm our hypothesis, BRB was experimentally broken by cryopexy, a well-established method to produce BRB breakdown.[31] Cryopexy was performed in the right eye of iron dextran-injected mice, whereas the left eye served as a control. BRB breakdown was confirmed by immunohistochemistry against serum albumin (Fig. 5D) and Evans Blue/bis-benzamide vascular leakage (Fig. 5E). Furthermore, Prussian blue staining showed iron leaking from the retinal vessels (Fig. 6A). One hour after cryopexy, ICP-MS was used to quantify total iron content in the retinal parenchyma. The results showed that iron was significantly increased in cryopexed retinas (2.755 ± 1.4 µg iron/g retina in control eyes, n = 4, vs. 12.052 ± 1.764 µg iron/g retina with cryopexy; n = 6; $P = 0.005$) (Fig. 6B), confirming that massive iron entry only occurs when BRB is compromised.

Ferritin Expression in the Retina Was Increased During Systemic Iron Overload Without Retinal Iron Overload

To understand why ferritin expression was increased while iron content and other iron handling proteins remained at normal levels in diabetic retinas, and to determine whether this was a specific finding that occurred in diabetic retinopathy, retinal ferritin and transferrin receptor expression four hours after iron dextran injection in WT mice was assessed by Western blot analysis. The results showed a 1.8-fold increased L-ferritin expression in the retinas of iron dextran-injected mice (0.595 ± 0.136 au in the saline solution–injected mice vs. 1.040 ± 0.071 au in the iron dextran-injected mice; n = 4; $P = 0.0272$) and no change for the transferrin receptor levels (1.151 ± 0.074 au in the saline solution–injected mice vs. 1.384 ± 0.097 au in the iron dextran-injected mice; n = 4; $P = 0.105$) (Fig. 7A). Furthermore, to confirm that ferritin was increased in the whole retinal parenchyma and not only in the endothelial cells in contact with the intravascular iron, an immunohistochemistry against L-ferritin and collagen IV was performed (Fig. 7B). The results obtained showed that L-ferritin expression was not accumulated in the endothelial cells, therefore confirming that systemic iron overload causes an increase of L-ferritin expression in the retinal parenchyma without BRB breakdown and retinal parenchyma iron increase.

Discussion

Previous reports have described the association between iron overload and diabetic retinopathy.[16,41] Our results showed that 20-week-old db/db mice had systemic iron overload and increased ferritin expression in the retina, which fully agree with the results observed by Chaudhary et al. in 2018.[23] However, unexpectedly, analysis of retinal iron by ICP-MS did not show higher iron content in the retina of

Investigative Ophthalmology & Visual Science

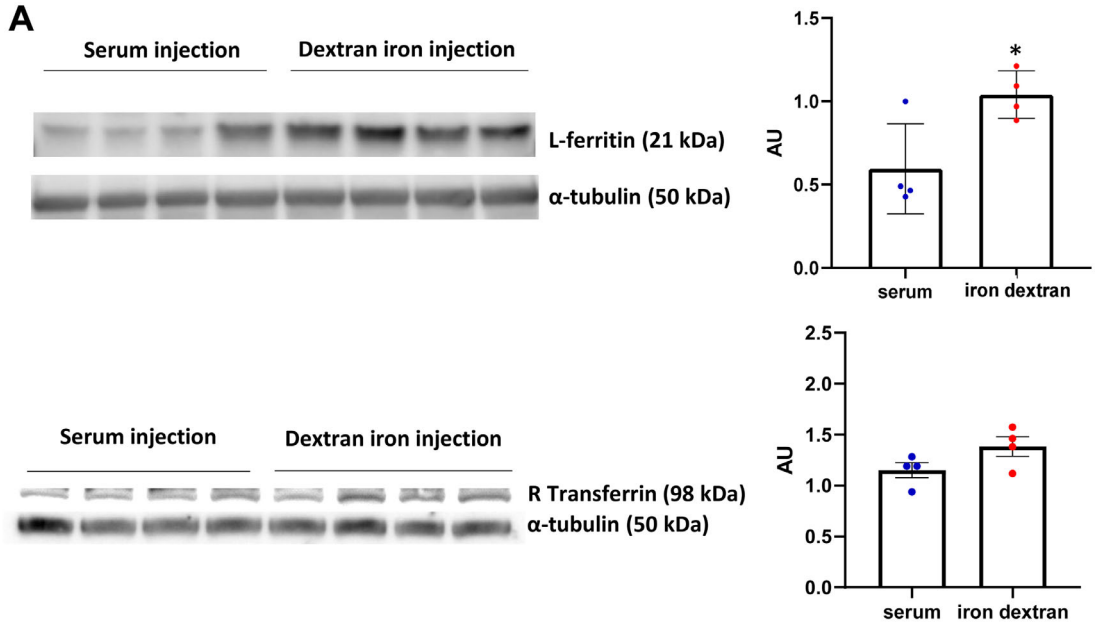

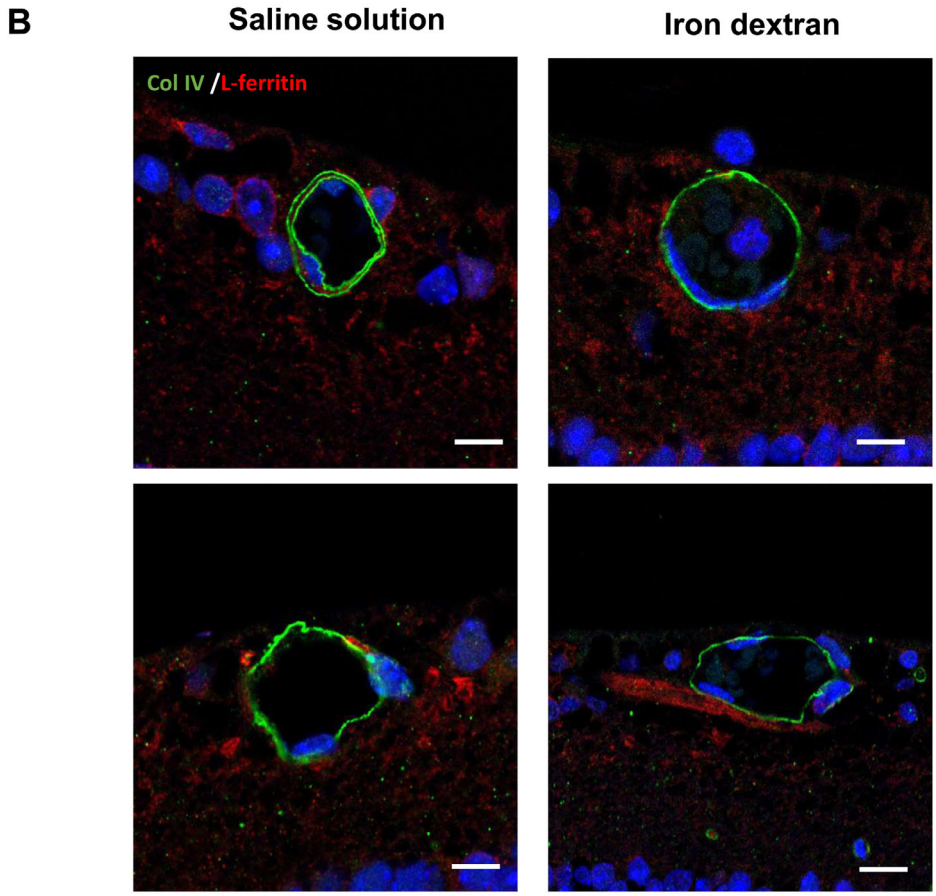

Figure 7. L-ferritin expression increased in retinas but not in endothelial cells of iron dextran-injected mice. (**A**) Western blot analysis revealed a significant 1.8-fold increase in L-ferritin expression in the retinas of mouse injected with iron dextran compared to the saline solution–injected controls, whereas transferrin receptor levels remained unchanged in these mice. α-tubulin was used as a loading control. *$P < 0.05$. (**B**) Immunohistochemistry against L-ferritin and collagen IV showed that L-ferritin expression was similar in saline solution injected mice and iron dextran-injected mice, indicating that L-ferritin was not being accumulated in vascular endothelial cells of iron dextran-injected mice. *Scale bar*: 7.35 µm.

diabetic mice. In addition, no changes were found in retinal iron import machinery of db/db mice, which supports the fact that retinal iron content was not increased.

Classical methods for iron detection, such as Prussian blue staining, are not sensitive enough to detect iron in the retina. There are high precision techniques to locate and quantify iron in the retina, such as particle-induced X-ray emission and synchrotron X-ray fluorescence (SXRF),[42,43] although these have a very limited access. ICP-MS is also a high sensitivity method for iron detection, and it is more available, but it does not provide information about the iron location within the retinal layers. Thus in situ detection of retinal iron can be challenging. For this reason, and because ferritin expression changes proportionally to iron levels in systemic tissues,[33] most studies use ferritin expression as an indirect indicator for retinal iron content,[23,24,44,45] justifying that an increase of ferritin expression in the retina is equivalent to retinal iron overload. Nevertheless, our results point out that ferritin expression might not always be a reliable marker to estimate iron content in the retina as it has been used so far.

We have shown that in diabetic mice with systemic iron overload, the retina remains protected from iron entry, at least until the age of 20 weeks, but how is the retina protected? In a recent study of long-term iron overload induced by iron dextran injections in mice,[24] BRB was proposed to prevent the retina from iron entry, so we next analyzed BRB status in db/db mice. BRB breakdown is a hallmark of diabetic retinopathy, and its breakage occurs as a consequence of different stresses, like hypoxia, oxidative damage and/or inflammation. BRB disruption has been linked to VEGF overexpression, endothelial tight junction alterations, and vascular leakage leading to retinal edema.[46] In or study, diabetic mice did no present any sign of BRB breakdown or any related alterations, suggesting an early stage of diabetic retinopathy in 20-week-old db/db mice. However, we can assume that, eventually, db/db mice will develop BRB breakdown and iron will enter in the retina, producing iron overload, as happened when we experimentally broke the BRB by cryopexy in iron dextran-injected mice. Altogether, the results obtained showed that in the retina a massive entrance of iron only occurs when BRB is compromised. This mechanism has been recently showed in the brain of aging mice with systemic iron overload, where, after blood brain barrier breakdown, the brain becomes unprotected and suffers iron overload.[47]

Signs of retinal alterations in db/db mice are reported to appear at variable stages of diabetic progression.[37,48–50] For instance, decrease of retinal thickness in db/db mice has been described to appear in 20-month-old individuals in some reports.[27,51] In contrast, our results did not show retinal thinning or thickening in 20-week-old mice, similar to the results published by Yang et al.,[52] where retinal thinning appeared later on. The upregulation of VEGF has also been reported in db/db retinas from 13-week-old mice.[48] However, our results did not reveal any increase in VEGF expression in 20-week-old mice, which is consistent with an unaltered BRB. The variability in the onset of lesions during diabetic retinopathy in mice could be explained by the different diets available among different animal facilities, because the administration of neuroprotective or antioxidant compounds present in the diet can delay the BRB disruption and related alterations.[53]

Another unexpected finding in our study was the overexpression of ferritin in the db/db mouse retinas without iron increase, whereas other iron-handling proteins remained unaltered. Ferritin levels are post-transcriptionally regulated by the so-called IRPs, which bind to ferritin mRNA and prevent its expression. When intracellular iron is high, IRPs lose the capacity to bind to ferritin mRNA, and thus ferritin levels increase.[54] As for the retina, this mechanism has been described using a model of IRP deficiency in which ferritin expression in the retina was increased.[55] In contrast, on iron overload, transferrin receptor mRNA is no longer protected by IRPs and becomes unstable to avoid more iron entrance. Surprisingly, retinas from db/db and iron dextran-injected mice, which had increased ferritin expression and no change in the transferrin receptor levels, did not present a higher iron content that could trigger IRP depletion and ferritin increase. This suggests the existence of a signaling mechanism between the retina and the rest of the body. The retina could be detecting systemic iron overload and activating ferritin synthesis as a compensatory response in front a potential BRB breakdown, given that a single ferritin complex can harbor up to 4500 molecules of iron and act as a natural iron chelator.[56]

Apart from sequestering deleterious free iron, ferritin is also overexpressed in chronic inflammatory diseases such as type 2 diabetes mellitus.[57] Ferritin induces anti-inflammatory cytokines and works as an immunomodulator, although this applies specially to H-ferritin.[58] Nevertheless, the fact that increased ferritin was present in both diabetic and iron dextran-injected mice retinas and that both models had systemic iron overload suggests that ferritin expression in the retina might be regulated by systemic iron excess.

All together our results demonstrated for the first time that ferritin expression cannot always be extrapolated to iron content in the retina. Diabetic mice with an intact BRB and systemic iron overload showed increased retinal ferritin, but no changes were found in iron content nor iron import machinery in the retina. In addition, systemic iron overload induced by an injection of iron dextran confirmed that retinal iron only increased when BRB was compromised. Overall, we hypothesized that the retina might be protected by, at least, two different autonomous mechanisms in front of systemic iron overload in diabetic retinopathy. The first limiting factor for iron entry would be the regulation at the BRB, and the second would be the increase of ferritin expression before BRB breakdown and retinal iron increase.

Monitoring iron in patients with type 2 diabetes is a common practice in the follow-up of the disease.[59] Our findings show that systemic iron overload appears before retinal iron overload, meaning that early detection and treatment with iron chelators could stop the passage of iron into the retina and prevent iron-induced retinal damage.

Acknowledgments

The authors truly thank Lorena Noya, Verónica Melgarejo, and Ángel Vázquez for their technical assistance.

Supported by the Ministerio de Ciencia e Innovación, Spain (grant number PID2021-122545OB-I00) and Fondo Europeo de Desarrollo Regional (FEDER).

Disclosure: **A. Bonet**, None; **J. Pampalona**, None; **E. Jose-Cunilleras**, None; **V. Nacher**, None; **J. Ruberte**, None

References

1. Abbaspour N, Hurrell R, Kelishadi R. Review on iron and its importance for human health. *J Res Med Sci*. 2014;19:164.

2. Yau KW, Baylor DA. Cyclic GMP-activated conductance of retinal photoreceptor cells. *Annu Rev Neurosci*. 1989;12:289–327.
3. Moiseyev G, Takahashi Y, Chen Y, et al. RPE65 is an iron(II)-dependent isomerohydrolase in the retinoid visual cycle. *J Biol Chem*. 2006;281:2835–2840.
4. Adijanto J, Du J, Moffat C, Seifert EL, Hurley JB, Philp NJ. The retinal pigment epithelium utilizes fatty acids for ketogenesis. *J Biol Chem*. 2014;289:20570–20582.
5. Mayle KM, Le AM, Kamei DT. The intracellular trafficking pathway of transferrin. *Biochim Biophys Acta*. 2012;1820:264.
6. Dunaief JL, Hahn P, Rouault T, Harris ZL. Retinal iron metabolism and its possible role in AMD pathogenesis. *Invest Ophthalmol Vis Sci*. 2004;45:2291–2291.
7. Chen TT, Li L, Chung DH, et al. TIM-2 is expressed on B cells and in liver and kidney and is a receptor for H-ferritin endocytosis. *J Exp Med*. 2005;202:955–965.
8. Li JY, Paragas N, Ned RM, et al. Scara5 is a ferritin receptor mediating non-transferrin iron delivery. *Dev Cell*. 2009;16:35–46.
9. Valença A, Mendes-Jorge L, Bonet A, et al. TIM2 modulates retinal iron levels and is involved in blood-retinal barrier breakdown. *Exp Eye Res*. 2021;202(October 2020):108292.
10. Mendes-Jorge L, Ramos D, Valença A, et al. L-ferritin binding to Scara5: A new iron traffic pathway potentially implicated in retinopathy. *PLoS One*. 2014;9(9):e106974.
11. Zhou ZD, Tan EK. Iron regulatory protein (IRP)-iron responsive element (IRE) signaling pathway in human neurodegenerative diseases. *Mol Neurodegener*. 2017;12(1):75.
12. Gray NK, Hentze MW. Iron regulatory protein prevents binding of the 43S translation pre-initiation complex to ferritin and eALAS mRNAs. *EMBO J*. 1994;13:3882–3891.
13. Meneghini R. Iron homeostasis, oxidative stress, and DNA damage. *Free Radic Biol Med*. 1997;23:783–792.
14. Zhao T, Guo X, Sun Y. Iron Accumulation and lipid peroxidation in the aging retina: Implication of ferroptosis in age-related macular degeneration. *Aging Dis*. 2021;12:529–551.
15. Hughes JM, Groot AJ, Van Groep P Der et al. Active HIF-1 in the normal human retina. *J Histochem Cytochem*. 2010;58:247.
16. Ciudin A, Hernández C, Simó R. Iron overload in diabetic retinopathy: A cause or a consequence of impaired mechanisms? *Exp Diabetes Res*. 2010;2010:714108.
17. Wu W, Yuan J, Shen Y, et al. Iron overload is related to elevated blood glucose levels in obese children and aggravates high glucose-induced endothelial cell dysfunction in vitro. *BMJ Open Diabetes Res Care*. 2020;8(1):e001426.
18. Misra G, Bhatter SK, Kumar A, Gupta V, Khan MY. Iron profile and glycaemic control in patients with type 2 diabetes mellitus. *Med Sci*. 2016;4(4):22.
19. Liu J, Li Q, Yang Y, Ma L. Iron metabolism and type 2 diabetes mellitus: A meta-analysis and systematic review. *J Diabetes Invest*. 2020;11:946–955.
20. Hahn P, Chen L, Beard JL, Harris ZL, Dunaief JL. Disruption of Ceruloplasmin and Hephaestin in mice causes retinal iron overload and retinal degeneration with features of age–related macular degeneration. *Invest Ophthalmol Vis Sci*. 2004;45:2292–2292.
21. Gnana-Prakasam JP, Ananth S, Prasad PD, et al. Expression and iron-dependent regulation of succinate receptor GPR91 in retinal pigment epithelium. *Invest Ophthalmol Vis Sci*. 2011;52:3751–3758.
22. Arjunan P, Gnanaprakasam JP, Ananth S, et al. Increased retinal expression of the pro-angiogenic receptor GPR91 via BMP6 in a mouse model of juvenile hemochromatosis. *Invest Ophthalmol Vis Sci*. 2016;57:1612–1619.
23. Chaudhary K, Promsote W, Ananth S, et al. Iron overload accelerates the progression of diabetic retinopathy in association with increased retinal renin expression. *Sci Rep*. 2018;8(1):3025.
24. Shu W, Baumann BH, Song Y, Liu Y, Wu X, Dunaief JL. Iron accumulates in retinal vascular endothelial cells but has minimal retinal penetration after IP iron dextran injection in mice. *Invest Ophthalmol Vis Sci*. 2019;60:4378–4387.
25. Belke DD, Severson DL. Diabetes in mice with monogenic obesity: The db/db mouse and its use in the study of cardiac consequences. *Methods Mol Biol*. 2012;933:47–57.
26. Burke SJ, Batdorf HM, Burk DH, et al. db/db Mice exhibit features of human type 2 diabetes that are not present in weight-matched C57BL/6J mice fed a western diet. *J Diabetes Res*. 2017;2017:8503754.
27. Bogdanov P, Corraliza L, Villena JA, et al. The db/db mouse: A useful model for the study of diabetic retinal neurodegeneration. *PLoS One*. 2014;9(5):e97302.
28. Musumeci M, Maccari S, Massimi A, et al. Iron excretion in iron dextran-overloaded mice. *Blood Transfus*. 2014;12:485.
29. Wichaiyo S, Yatmark P, Morales Vargas RE, et al. Effect of iron overload on furin expression in wild-type and β-thalassemic mice. *Toxicol Reports*. 2015;2:415–422.
30. Robinson R, Barathi VA, Chaurasia SS, Wong TY, Kern TS. Update on animal models of diabetic retinopathy: From molecular approaches to mice and higher mammals. *DMM Dis Model Mech*. 2012;5:444–456.
31. Derevjanik NL, Vinores SA, Xiao WH, et al. Quantitative assessment of the integrity of the blood-retinal barrier in mice. *Invest Ophthalmol Vis Sci*. 2002;43:2462–2467.
32. Goebel W, Kretzchmar-Gross T. Retinal thickness in diabetic retinopathy: A study using optical coherence tomography (OCT). *Retina*. 2002;22:759–767.
33. Daru J, Colman K, Stanworth SJ, De La Salle B, Wood EM, Pasricha SR. Serum ferritin as an indicator of iron status: What do we need to know? *Am J Clin Nutr*. 2017;106(Suppl 6):1634S–1639S.
34. Munro HN. Iron regulation of ferritin gene expression. *J Cell Biochem*. 1990;44:107–115.
35. Wang J, Pantopoulos K. Regulation of cellular iron metabolism. *Biochem J*. 2011;434(Pt 3):365.
36. Faruqi A, Mukkamalla SKR. Iron binding capacity. In: *StatPearls* [Internet]. Treasure Island, FL: StatPearls Publishing; 2022. Available from: https://www.ncbi.nlm.nih.gov/books/NBK559119/.
37. Cheung AKH, Fung MKL, Lo ACY, et al. Aldose reductase deficiency prevents diabetes-induced blood-retinal barrier breakdown, apoptosis, and glial reactivation in the retina of db/db mice. *Diabetes*. 2005;54:3119–3125.
38. Boyer DS, Hopkins JJ, Sorof J, Ehrlich JS. Anti-vascular endothelial growth factor therapy for diabetic macular edema. *Ther Adv Endocrinol Metab*. 2013;4(6):151–169.
39. Campbell M, Humphries P. The blood-retina barrier tight junctions and barrier modulation. *Adv Exp Med Biol*. 2013;763:70–84.
40. Tian R, Luo Y, Liu Q, et al. The effect of claudin-5 overexpression on the interactions of claudin-1 and -2 and barrier function in retinal cells. *Curr Mol Med*. 2014;14:1226–1237.
41. Gnana-Prakasam JP, Chaudhary K, Promsote W, et al. Retinal iron overload during diabetic retinopathy accelerates ganglion cell death. *Invest Ophthalmol Vis Sci*. 2016;57:751–751.
42. Ugarte M, Grime GW, Osborne NN. Distribution of trace elements in the mammalian retina and cornea by use of particle-induced X-ray emission (PIXE): Localisation of zinc does not correlate with that of metallothioneins. *Metallomics*. 2014;6:274–278.

Investigative Ophthalmology & Visual Science

43. Ugarte M, Grime GW, Lord G, et al. Concentration of various trace elements in the rat retina and their distribution in different structures. *Metallomics*. 2012;4:1245–1254.
44. Hahn P, Qian Y, Dentchev T, et al. Disruption of ceruloplasmin and hephaestin in mice causes retinal iron overload and retinal degeneration with features of age-related macular degeneration. *Proc Natl Acad Sci*. 2004;101:13850–13855.
45. Zhao L, Li Y, Song D, et al. A high serum iron level causes mouse retinal iron accumulation despite an intact blood-retinal barrier. *Am J Pathol*. 2014;184:2862–2867.
46. Zhang X, Zeng H, Bao S, Wang N, Gillies MC. Diabetic macular edema: New concepts in patho-physiology and treatment. *Cell Biosci* 2014;4:1–14.
47. Mezzanotte M, Ammirata G, Boido M, Stanga S, Roetto A. BBB damage in aging causes brain iron deposits via astrocyte-neuron crosstalk and Hepc/Fpn1 pathway. *bioRxiv*. 2021:2021–07.
48. Li J, Wang JJ, Yu Q, Chen K, Mahadev K, Zhang SX. Inhibition of reactive oxygen species by lovastatin downregulates vascular endothelial growth factor expression and ameliorates blood-retinal barrier breakdown in db/db mice. *Diabetes*. 2010;59:1528–1538.
49. Xiong SQ, Jiang HB, Xu HZ, Xia XB. Effect of pyridone agent on blood-retinal barrier in diabetic mice. *Int J Ophthalmol*. 2017;10:890–895.
50. Kim J, Kim C-S, Lee IS, et al. Extract of Litsea japonica ameliorates blood–retinal barrier breakdown in db/db mice. *Endocrine*. 2014;46:462–469.
51. Sheskey SR, Antonetti DA, Rentería RC, Lin CM. Correlation of retinal structure and visual function assessments in mouse diabetes models. *Invest Ophthalmol Vis Sci*. 2021;62(10):20.
52. Yang Q, Xu Y, Xie P, et al. Retinal neurodegeneration in db/db mice at the early period of diabetes. *J Ophthalmol*. 2015;2015:757412.
53. Rossino MG, Dal Monte M, Casini G. Relationships between neurodegeneration and vascular damage in diabetic retinopathy. *Front Neurosci*. 2019;13:1172.
54. Hentze MW, Kühn LC. Molecular control of vertebrate iron metabolism: mRNA-based regulatory circuits operated by iron, nitric oxide, and oxidative stress. *Proc Natl Acad Sci USA*. 1996;93:8175.
55. Hahn P, Dentchev T, Qian Y, Rouault T, Harris ZL, Dunaief JL. Immunolocalization and regulation of iron handling proteins ferritin and ferroportin in the retina. *Mol Vis*. 2004;10:598–607.
56. Aisen P, Enns C, Wessling-Resnick M. Chemistry and biology of eukaryotic iron metabolism. *Int J Biochem Cell Biol*. 2001;33:940–959.
57. Ferńandez-Real JM, Mcclain D, Review MM. Mechanisms linking glucose homeostasis and iron metabolism toward the onset and progression of type 2 diabetes. *Diabetes Care*. 2015;38:2169–2176.
58. Kernan KF, Carcillo JA. Hyperferritinemia and inflammation. *Int Immunol*. 2017;29:401.
59. Saha S, Murgod R. Evaluation of iron profile in type II diabetes mellitus cases. *Int J Biotechnol Biochem*. 2019;15:27–37.